



저작자표시-비영리-변경금지 2.0 대한민국

이용자는 아래의 조건을 따르는 경우에 한하여 자유롭게

- 이 저작물을 복제, 배포, 전송, 전시, 공연 및 방송할 수 있습니다.

다음과 같은 조건을 따라야 합니다:



저작자표시. 귀하는 원저작자를 표시하여야 합니다.



비영리. 귀하는 이 저작물을 영리 목적으로 이용할 수 없습니다.



변경금지. 귀하는 이 저작물을 개작, 변형 또는 가공할 수 없습니다.

- 귀하는, 이 저작물의 재이용이나 배포의 경우, 이 저작물에 적용된 이용허락조건을 명확하게 나타내어야 합니다.
- 저작권자로부터 별도의 허가를 받으면 이러한 조건들은 적용되지 않습니다.

저작권법에 따른 이용자의 권리는 위의 내용에 의하여 영향을 받지 않습니다.

이것은 [이용허락규약\(Legal Code\)](#)을 이해하기 쉽게 요약한 것입니다.

[Disclaimer](#)

의학박사 학위논문

p53 및 Ki-67 발현을 이용한 구강과 후두 전암성 및  
악성 병변 진단을 위한 예측 모형 구축에 관한 연구

Predictive modeling for the diagnosis of oral and  
laryngeal premalignant and malignant lesions  
using expression of p53 and Ki-67

울 산 대 학 교 대 학 원

의 학 과

정 지 선

p53 및 Ki-67 발현을 이용한 구강과 후두 전암성 및  
악성 병변 진단을 위한 예측 모형 구축에 관한 연구

지도교수 송 준 선

이 논문을 의학박사 학위 논문으로 제출함

2022 년 8 월

울 산 대 학 교 대 학 원

의 학 과

정 지 선

정지선의 의학박사학위 논문을 인준함

심사위원    조 경 자    인

심사위원    송 준 선    인

심사위원    이 윤 세    인

심사위원    이 희 진    인

심사위원    노    진    인

울 산 대 학 교 대 학 원

2022 년 8 월

## Abstract

### Background

Oral and laryngeal epithelial lesions are diagnosed based on histologic criteria of WHO classification which may cause interobserver variability. Integrated diagnostic approach based on immunohistochemistry (IHC) is required that can help the interpretation of ambiguous histological findings of epithelial lesions.

### Methods

The oral cavity and larynx tissues of 114 cases from 104 patients were examined by IHC for p53 and Ki-67. Logistic regression analysis and decision tree algorithm were employed to develop the scoring system and predictive model for differentiating the epithelial lesions. Cohen kappa coefficient was conducted to evaluate the interobserver variability. The comparison between *TP53* mutation and expression patterns of p53 was conducted by next-generation sequencing (NGS) and IHC.

### Results

Two expression patterns for p53, diffuse expression type (pattern HI) and null type (pattern LS), and pattern HI for Ki-67 were significantly associated with high grade dysplasia (HGD) or squamous cell carcinoma (SqCC). With accuracy and *the area under* a receiver operating characteristic curve (AUC) of 84.6% and 0.85, respectively, the scoring system based on p53 and Ki-67 classified epithelial lesions into two types: non-dysplasia (ND) or low grade dysplasia (LGD), and HGD or SqCC. The decision tree model using p53 and Ki-67 classified epithelial lesions into ND, LGD, and group 2 including HGD or SqCC with accuracy and AUC of 75% and 0.87, respectively. The integrated diagnosis had a better correlation with near perfect agreement (weighted kappa 0.92, unweighted kappa 0.88). The patterns HI and LS for p53 were confirmed to be correlated with

missense mutations and nonsense/frameshift mutations, respectively.

### **Conclusions**

The correlation between the *TP53* mutation and the expression patterns of p53 was confirmed and the predictive model of diagnosis was developed. Therefore, the scoring system based on p53 and Ki-67 expression patterns aids the differentiation of epithelial lesions, especially when the morphologic features are ambiguous.

**Keywords:** oral dysplasia, laryngeal dysplasia, squamous cell carcinoma, p53, Ki-67

## Contents

Abstract .....	i
Contents .....	iii
List of Tables .....	iv
List of Figures .....	v
Introduction .....	1
Materials and Methods .....	3
1. Study samples .....	3
2. Immunohistochemistry.....	4
3. DNA extraction .....	7
4. Targeted NGS .....	8
5. Bioinformatics analysis .....	8
6. Establishment of decision tree model .....	9
7. Statistical analysis .....	9
Results .....	11
Discussion .....	24
Conclusion .....	31
References .....	32
Korean Abstract .....	38

## List of Tables

Table 1. Clinicopathologic features of cases. ....	12
Table 2. Comparison of two groups: LD and LGD, HGD and SqCC.....	14
Table 3. Univariate and multivariate analysis of p53 and Ki-67 for predicting HGD and SqCC. ....	15
Table 4. Parameters and scoring points of scoring system. ....	16
Table 5. Comparisons of the classification efficiency of the two cut-off points. ....	17
Table 6. Kappa scores for diagnosis based on H&E slide and the integrated diagnosis .....	19
Table 7. <i>TP53</i> mutation in SqCC. ....	21



## List of Figures

Figure 1. The representative image of squamous epithelial lesions. ....	5
Figure 2. p53 IHC staining patterns. ....	6
Figure 3. Ki-67 IHC staining pattern ....	6
Figure 4. p53 and Ki-67 IHC staining pattern of SqCC ....	7
Figure 5. Variable importance in logistic regression analysis. ....	16
Figure 6. The mean and AUC of two groups for a scoring system: ND or LGD, HGD or SqCC. ....	17
Figure 7. Decision tree models to differentiate epithelial lesion. ....	18
Figure 8. Changes between diagnosis based on H&E slide and the integrated diagnosis. ....	20
Figure 9. Comprehensive <i>TP53</i> genomic profile of SqCC. ....	21
Figure 10. Disease free survival of SqCC and HGD according to p53 expression patterns ....	23
Figure 11. The first case of discrepancy between diagnosis based on H&E slide and classification by decision tree model. ....	28
Figure 12. The second case of discrepancy between diagnosis based on H&E slide and classification by decision tree model. ....	29
Figure 13. The third case of discrepancy between diagnosis based on H&E slide and classification by decision tree model. ....	29
Figure 14. The fourth case of discrepancy between diagnosis based on H&E slide	

and classification by decision tree model. .... 30

## Introduction

*TP53* gene is the most frequently altered gene in head and neck squamous cell carcinoma (HNSCC), including oral cavity and larynx. Next-generation sequencing (NGS) confirmed the prevalence of *TP53* mutation ranges 30 – 70% (1, 2). It often appears in squamous dysplasia, a premalignant lesion, suggesting that it occurs in early stage of carcinogenesis. As a predictor and prognostic marker, *TP53* mutation is related with poor prognosis and resistance to chemotherapy and radiotherapy (1, 3).

Through analyzing the correlation between *TP53* mutation and expression of p53 protein, immunohistochemistry (IHC) can effectively detect *TP53* genomic alteration status for a more accurate diagnosis. Several studies have analyzed *TP53* mutation and the expression of p53 protein in the epithelial lesion of the oral cavity and larynx (4-8). Recently, Sawada *et al.* confirmed the correlation between *TP53* genetic alteration and p53 protein by NGS, fluorescence *in situ* hybridization analysis (FISH), and IHC in oral epithelial dysplasia. They categorized the results of IHC for p53 into four patterns and identified that two patterns, diffuse expression type (pattern HI) and null type (pattern LS) are significantly related to *TP53* mutation, especially missense mutation and nonsense mutation, respectively (9).

HNSCC including oral cavity and larynx squamous cell carcinoma (SqCC) is the sixth most common malignancy worldwide. Despite improved multimodal approach including surgery, chemotherapy, and radiotherapy, survival of patients with HNSCC is not significantly increased. Early detection of HNSCC and its premalignant lesion is important because it can improve not only survival rate, but also the health-related quality of life of patients, given the anatomical

complexity and daily function of head and neck region (10).

World Health Organization (WHO) classification provides diagnostic criteria based on the presence of histologic features for oral and laryngeal epithelial dysplasia (11). The criteria include the architectural and cytologic features, several of which are imprecise, resulting in subjective evaluation and interobserver variability (12-16). Some histologic features can be also observed in reactive lesions including edges of ulcers, candida infection, and mucosal changes following chemotherapy, which may mimic dysplasia (16, 17). In comparison to surgical samples, accurate histological evaluation of biopsy specimens can be difficult due to inflammation or inadequate tissue processing, such as embedding (18).

To aid more accurate diagnosis based on histologic criteria, many reports studied prognostic and predictor markers including p53 and proliferative index marker Ki-67 as new ancillary techniques (19-21). However, no integrated diagnostic model to improve the accuracy has been reported. Herein, I analyzed the expression patterns of p53 and Ki-67 in oral and laryngeal epithelial lesions including non-dysplasia (ND), low grade dysplasia (LGD), high grade dysplasia (HGD), and SqCC, and conducted *TP53* mutational screening by NGS for developing the diagnostic model that allows early and precise diagnosis of epithelial dysplasia.

## Materials and methods

### Study samples

The study cohort consisted of 104 patients treated with biopsy or surgery for squamous epithelial lesion including ND, LGD, HGD, and SqCC from January 2018 to September 2021 at Asan Medical Center (Seoul, Republic of Korea). 114 cases of 104 patients were available for the analysis. Among the 104 patients, the tissues of 96 patients were obtained only once, the tissues of six patients were obtained twice, and the tissues of two patients were obtained three times. NGS was performed on sixteen of 114 previously stated cases.

To assess interobserver variability, two pathologists (J.S.S and J.S.J) independently evaluated each slide. The pathologists were blinded to the patient's diagnosis and clinical information. To reconfirm the diagnosis, all hematoxylin and eosin (H&E) stained sections were pathologically reviewed by two head and neck expert pathologists (K.J.C and J.S.S) and one resident pathologist (J.S.J). Squamous dysplasia of oral cavity and larynx were graded using a binary system suggested by Kujan O *et al.* (22) and the 2017 WHO Tumor Classification criteria (11), respectively. The final diagnosis was reconfirmed using histologic features and the results of IHC staining. Disagreement between pathologists was resolved by a consensus meeting. The representative images of squamous epithelial lesions are shown in Fig.1.

Patient's clinicopathological information including demographics and characteristics of patients, diagnosis, follow-up period, and time to recurrence were obtained from electronic medical records and surgical pathology reports. The recurrence of SqCC or HGD was defined as the occurrence of SqCC or HGD in the same site within the follow-up period following active treatment (i.e.,

surgical excision or laryngeal microsurgery) through imaging analysis with/without pathologic confirmation. Smoking history was quantified in packs – years and patients were classified as non-smokers, former smokers who quit more than ten years ago, and current smokers. Alcohol consumption is defined as the absence of a history of alcohol use, the consumption of three or fewer cups of alcohol per day, or the consumption of more than three cups per day. This study was performed according to the protocol approved by Institutional Review Board of Asan Medical Center (2021-0681).

### **Immunohistochemistry**

IHC analysis for p53 and Ki-67 was performed. Immunohistochemical staining was performed using an automated staining system (BenchMark XT, Ventana Medical Systems, Tucson, AZ, USA) with antibodies for p53 (clone DO-7, DAKO, Glostrup, Denmark, 1:1000) and Ki-67 (clone MIB1, DAKO, Glostrup, Denmark, 1:200).

The IHC results were assessed using methods proposed by Sawada *et al* (9). They analyzed correlation between *TP53* genetic alteration and p53 expression pattern by NGS, FISH, and IHC. The IHC results for p53 were classified into four patterns: pattern NM (Normal), pattern BP (Basal and Parabasal), pattern HI (High), and pattern LS (Loss). The representative cases were shown in Fig. 2. In the pattern NM (Fig. 2A) and BP (Fig. 2B), the cells immunoreactive for p53 were restricted to basal and parabasal layers which is similar to expression pattern of normal epithelium. There was cutoff value at 50% positivity for p53 to discriminate patterns NM and BP (NM <50%; BP ≥50%). If the cells are immunoreactive for p53 extended beyond the basal and parabasal layers to the superficial layer, the pattern HI was determined (Fig. 2C). The pattern LS was a

complete loss of expression for p53 in the lesion (Fig. 2D). For SqCC, the basal layer was regarded as the peripheral cells of the invasive carcinoma nest, the parabasal layer corresponded to the upper layer of the peripheral cells, and the superficial layer corresponded to layers above the two layers (Fig. 4A-C).

The IHC staining results for Ki-67 were also categorized in the way described above except pattern LS which was not found in Ki-67 IHC. Unlike the results of p53, loss of expression for Ki-67, regarded as the pattern LS, was not identified (Fig. 3, 4D-E).

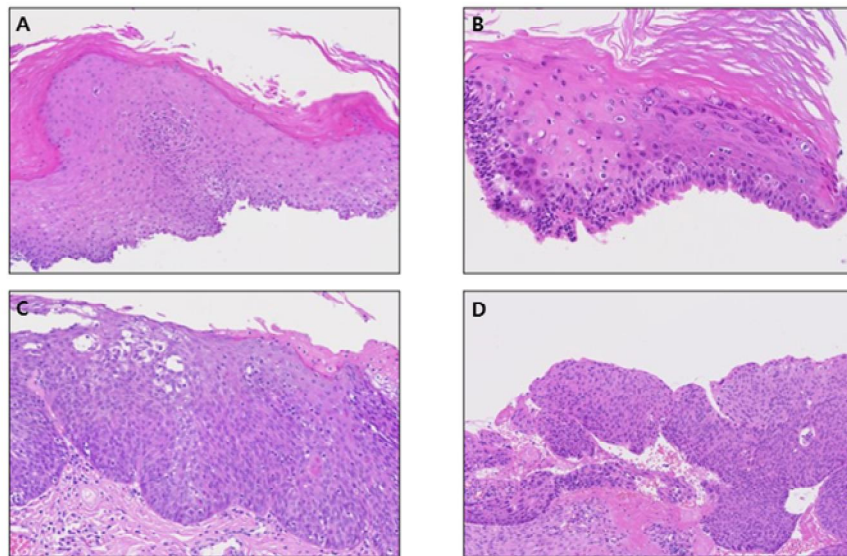


**Figure 1. The representative images of squamous epithelial lesions.** A. Non-dysplasia (ND), 10X. B. Low grade dysplasia (LGD), 20X. C. High grade dysplasia (HGD), 20X. D. Squamous cell carcinoma (SqCC), 10X.

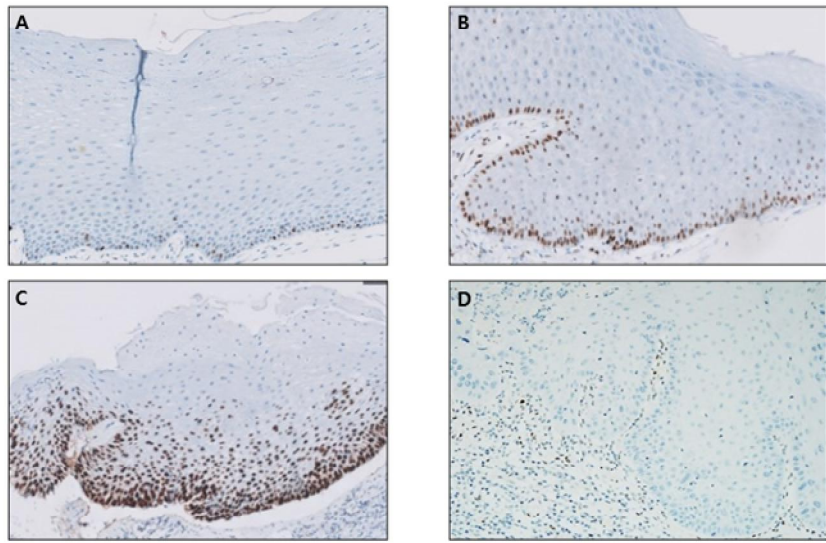


**Figure 2. p53 IHC staining patterns.** Representative results of p53 IHC staining. A. Pattern NM: p53-positive cells are distributed in the basal or parabasal layer (<50% of cells in basal or parabasal layer) B. Pattern BP: p53-positive cells are widely distributed in the basal or parabasal layer ( $\geq 50\%$ ). C. Pattern HI: p53-positive cells are diffusely located in more than three layers. D. Pattern LS: the lesion is immunonegative for p53. Images are viewed at a magnification of 10X (A&B) and 20X (C&D). IHC, immunohistochemistry.

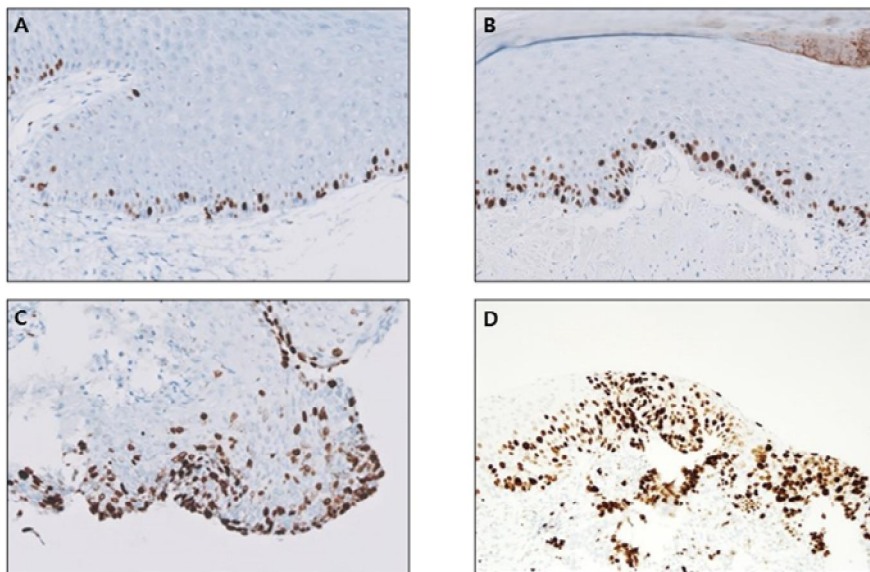




**Figure 3. Ki-67 IHC staining patterns.** Representative results of Ki-67 IHC staining. A. Pattern NM: Ki-67 positive cells are distributed in the basal or parabasal layer (<50% of cells in basal or parabasal layer) B. Pattern BP: Ki-67 positive cells are widely distributed in the basal or parabasal layer ( $\geq 50\%$ ). C&D. Pattern HI: Ki-67-positive cells are diffusely located in more than three layers. Images are viewed at a magnification of 10X (A&B) and 20X (C&D). IHC, immunohistochemistry.

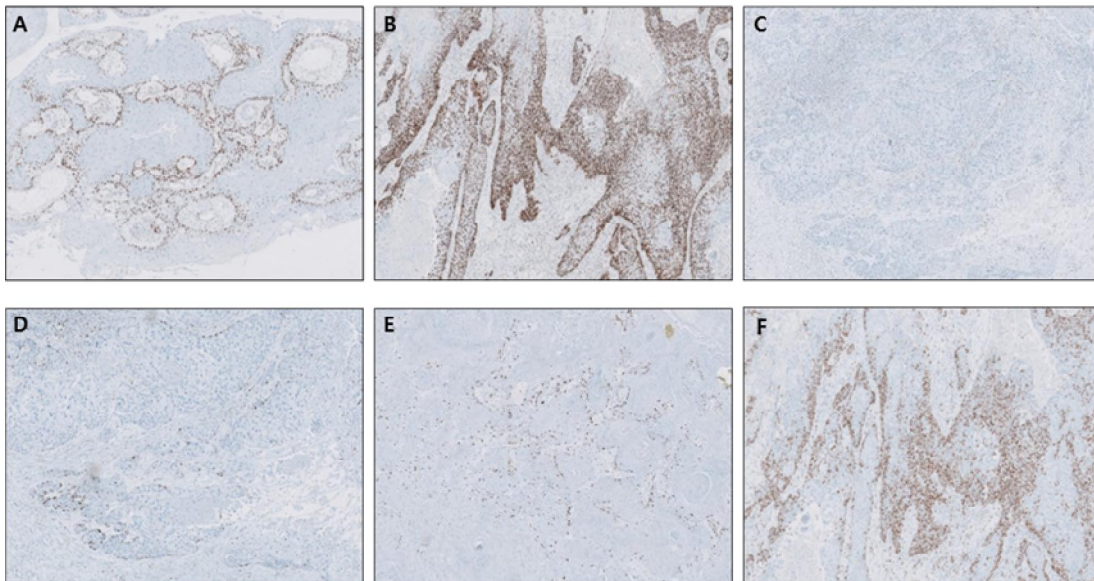


**Figure 4. p53 and Ki-67 IHC staining patterns of SqCC.** Representative results of p53 IHC staining (A-C). A. Pattern BP. B. Pattern HI. C. Pattern LS. C&D. Representative results of Ki-67 IHC staining (D-E). D. Pattern NM. E. Pattern BP. F. Pattern HI. Images are viewed at a magnification of 5X. SqCC, squamous cell carcinoma. IHC, immunohistochemistry.

### DNA extraction

Genomic DNA was extracted from the SqCC component in formalin-fixed

paraffin-embedded tissue (FFPE) samples after review of the matched hematoxylin/eosin-stained slides from each FFPE tissue section. Each tissue was deparaffinized with xylene and ethanol, and genomic DNA was isolated using NEXprep FFPE Tissue Kit (#NexK-9000; Geneslabs, Seongnam, Korea), in accordance with the manufacturer's recommendations. The tissue pellet was lysed completely during incubation with proteinase K in lysis buffer overnight at 56°C and further incubated for 3 min with magnetic beads and solution A at room temperature. After incubation for 5 min on a magnetic stand, the supernatant was removed and the beads were rinsed three times with ethanol. The beads were dried for 5 min, and the DNA was eluted in 50 µl of DNase-free and RNase-free water and quantified with a Quant-iT PicoGreen dsDNA Assay Kit (Invitrogen, Carlsbad, CA, USA).

### **Targeted NGS**

Targeted NGS was conducted on the MiSeq platform (Illumina, San Diego, CA, USA) with OncoPanel AMC version 4.0 for capture of the exons of 323 cancer-related genes [225 genes for single nucleotide variation (SNV) / insertion and deletion (INDEL) and copy number variation (CNV)] and partial introns from six genes that are commonly rearranged in cancer (23). Additional information about our in-house panel has been described elsewhere (24, 25).

### **Bioinformatics analysis**

Sequenced reads were aligned to the human reference genome (NCBI build 37) with the Burrows–Wheeler Aligner (0.5.9) (26). Demultiplexing was conducted with Mark Duplicates of the Picard package to remove polymerase chain reaction duplicates from the aligned read (<http://broadinstitute.github.io/picard>).

Deduplicated reads were realigned at known indel positions with GATK IndelRealigner (27). Base qualities were then recalibrated with GATK Table Recalibration. Somatic variant calling for single-nucleotide variants and short indels was conducted with MuTect (1.1.7) (28) and Somatic Indelocator in GATK, respectively. Common germline variants from candidates of somatic variants were filtered out with common dbSNP (build 141; found in  $\geq 1\%$  of samples) (29). Ultimate somatic variants were annotated with Variant Effect Predictor (version79) (30) and converted to MAF files with vcf2 maf (<https://github.com/mskcc/vcf2maf>). Somatic mutation signatures were inferred with the R package (31). Significantly mutated genes were identified with MutSig2CV (32). Somatic mutations were loaded and plotted in local cBioPortal (33). Copy number analyses were performed with CNVkit (34).

### **Establishment of decision tree model**

To construct a predictive model to distinguish squamous epithelial lesions, a decision tree model was constructed using the decision tree model algorithm in party package of R program; on R-4.1.3, caret-6.0.19. This algorithm selects a variable and divides into two groups until each impurity is minimized based on information gain. K-Fold cross validation was used to evaluate the decision tree models (35). The data was divided to train with probability of 0.7 (84 cases of train set) and validation set with probability of 0.3 (34 cases of test set). The training set was trained on the module of rpart method in caret package. The diagnostic ability of predictor model was evaluated by the accuracy, the area under the receiver operating characteristic curve (AUC), sensitivity, and specificity.

### **Statistical analysis**

Statistical analysis was conducted using R program (version 4.1.3, The R Foundation for Statistical Computing). Spearman correlation between p53 and Ki-67 expression pattern was computed. I grouped squamous epithelial lesions (ND, LGD, HGD, and SqCC) into two groups (ND and LGD; HGD and SqCC) and used Pearson chi-squared test. Univariate and multivariate logistic regression analyses were performed to compare the two groups. The results are shown as odds ratios (OR) with 95% confidence intervals (95% CI). Wilcoxon rank sum test was computed for comparing the average of two groups. To determine the optimal cut-off value, accuracy, AUC, sensitivity, and specificity were computed. Cohen kappa coefficient was conducted to evaluate the interobserver variability. Kaplan–Meier curve and log-rank test were conducted to evaluate the univariate association between p53 expression patterns and recurrence. Statistical significance was defined as a *P* value < 0.05.

## Results

### Clinicopathologic features

The clinicopathologic features of the 107 patients (114 cases) are summarized in Table 1. The patients comprised 91 (79.8%) men and 23 (20.2%) women with mean age of 62.4 years (median, 64.0 years; range, 23–84 years). Fifty-four cases were laryngeal epithelial lesions, and 60 cases were oral epithelial lesions. Of the total 114 cases, 26 (22.8%) cases were diagnosed with ND, 33 (28.9%) with LGD, 26 (22.8%) with HGD, and 29 (25.4%) with SqCC. Five of eight patients whose specimens were obtained more than twice had the same diagnosis, except for three patients.

When immunohistochemical results for p53 were analyzed, pattern NM which was similar with the staining pattern of normal epithelial lesion was detected in 21 of 26 cases (80.8%) of ND, while pattern NM was detected in six of 33 cases (18.2%) with LGD, three of 26 cases (11.5%) HGD, and was not detected in SqCC, respectively. Although pattern HI was significantly related with *TP53* mutation confirmed by Sawada *et al.* (9), it was detected in one of 26 cases (3.8%) in ND. Interestingly pattern HI and LS were detected in 17 of 33 cases (51.5%) with LGD, 22 of 26 cases (84.6%) in HGD, and 27 of 29 cases (93.1%) in SqCC. In brief, pattern NM appears most frequently in normal, and the frequency of this pattern decreases as the degree of dysplasia increases, whereas in pattern HI and LS, the frequency of this pattern increases as the degree of dysplasia increases.

The IHC staining results for Ki-67 was also analyzed by the same method as p53. In a total of 114 cases, pattern NM was detected in ten cases (8.8%), pattern BP was detected in 40 cases (35.1%), and pattern HI was detected in 64 cases (56.1%). Pattern NM or BP were detected in 24 of 26 cases (92.3%) in ND, 14 of

33 cases (42.4%) in LGD, three of 26 cases (11.5%) in HGD, and 10 of 29 cases (34.5%) in SqCC. Pattern HI was detected in two of 29 cases (7.7%) in ND, but increased to 19 of 33 cases (57.6%) in LGD, 23 of 26 cases (88.5%) in HGD, and 19 of 29 cases (65.5%) in SqCC. There was very weak linear relationship between p53 and Ki-67 expression patterns (Spearman's correlation coefficient value = 0.39;  $P < 0.001$ )

**Table 1. Clinicopathologic features of cases.**

	<b>ND (N=26)</b>	<b>LGD (N=33)</b>	<b>HGD (N=26)</b>	<b>SqCC (N=29)</b>	<b>Overall (N=114)</b>
<b>Age (yr)</b>					
Mean (SD)	57.1 (9.78)	63.0 (10.4)	66.4 (8.97)	62.9 (14.6)	62.4 (11.5)
<b>Gender</b>					
Male	23 (88.5%)	25 (75.8%)	19 (73.1%)	24 (82.8%)	91 (79.8%)
Female	3 (11.5%)	8 (24.2%)	7 (26.9%)	5 (17.2%)	23 (20.2%)
<b>Location</b>					
Larynx	9 (34.6%)	21 (63.6%)	15 (57.7%)	9 (31.0%)	54 (47.4%)
Oral cavity	17 (65.4%)	12 (36.4%)	11 (42.3%)	20 (69.0%)	60 (52.6%)
<b>Tobacco use</b>					
Non-smoker	9 (34.6%)	9 (27.3%)	11 (42.3%)	11 (37.9%)	40 (35.1%)
≤ 3 drinks per day	6 (23.1%)	14 (42.4%)	8 (30.8%)	7 (24.1%)	35 (30.7%)
> 3 drinks per day	11 (42.3%)	10 (30.3%)	7 (26.9%)	11 (37.9%)	39 (34.2%)
<b>Alcohol consumption</b>					
No history	8 (30.8%)	16 (48.5%)	16 (61.5%)	15 (51.7%)	55 (48.2%)
≤ 3 drinks per day	6 (23.1%)	9 (27.3%)	3 (11.5%)	7 (24.1%)	25 (21.9%)
> 3 drinks per day	12 (46.2%)	8 (24.2%)	7 (26.9%)	7 (24.1%)	34 (29.8%)
<b>BMI</b>					
Mean (SD)	23.2 (2.82)	25.0 (3.36)	24.0 (4.30)	23.1 (4.59)	23.9 (3.86)
<b>DM</b>					
Yes	8 (30.8%)	7 (21.2%)	8 (30.8%)	8 (27.6%)	31 (27.2%)
No	18 (69.2%)	26 (78.8%)	18 (69.2%)	21 (72.4%)	83 (72.8%)
<b>p53</b>					
Pattern NM	21 (80.8%)	6 (18.2%)	3 (11.5%)	0 (0%)	28 (24.6%)

Pattern BP	4 (15.4%)	10 (30.3%)	1 (3.8%)	2 (6.9%)	19 (16.7%)
Pattern HI	1 (3.8%)	13 (39.4%)	17 (65.4%)	22 (75.9%)	53 (46.5%)
Pattern LS	0 (0%)	4 (12.1%)	5 (19.2%)	5 (17.2%)	14 (12.3%)
<b>Ki-67</b>					
Pattern NM	6 (23.1%)	2 (6.1%)	0 (0%)	2 (6.9%)	10 (8.8%)
Pattern BP	18 (69.2%)	12 (36.4%)	3 (11.5%)	8 (27.6%)	40 (35.1%)
Pattern HI	2 (7.7%)	19 (57.6%)	23 (88.5%)	19 (65.5%)	64 (56.1%)

ND: non-dysplasia; LGD: low grade dysplasia; HGD: high grade dysplasia; SqCC: squamous cell carcinoma; SD: standard deviation; DM: diabetes mellitus.

### **Logistic regression analysis for differentiation of two groups: ND or LGD, HGD or SqCC**

Given the low risk of malignant transformation in LGD, squamous epithelial lesions were divided into two groups: group 1 (ND or LGD) and group 2 (HGD or SqCC) (36, 37). When two groups were compared on the basis of their clinicopathologic characteristics, the expression patterns of p53 ( $P < 0.001$ ) and Ki-67 ( $P < 0.001$ ) were significantly different (Table 2).

The univariable and multivariable logistic regression analysis of the p53 and Ki-67 expression patterns was conducted to develop a predictive model, and the results are summarized in Table 3. Univariable analysis revealed that the patterns HI (OR: 18.00, 95% CI = 4.28-75.69,  $P < 0.001$ ) and LS (OR: 9.00, 95% CI = 1.55-52.27,  $P = 0.014$ ) were significant predictors of group 2. The pattern HI of Ki-67 (OR: 18.86, 95% CI = 2.15-165.28,  $P = 0.008$ ) was also significantly associated with group 2.

Multivariate analysis revealed that the pattern HI (OR: 8.68, 95% CI = 1.84-40.98,  $P = 0.006$ ) and LS (OR: 7.66, 95% CI = 1.12-52.53,  $P = 0.038$ ) were significantly

related with group 2. The pattern HI of Ki-67 (OR: 10.63, 95% CI = 1.00-112.41,  $P = 0.049$ ) was also significantly associated with group 2.

**Table 2. Comparison of two groups: LD or LGD and HGD or SqCC.**

	<b>ND &amp; LGD (%) (n= 59)</b>	<b>HGD &amp; SqCC (%) (n= 55)</b>	<b><i>P</i> value</b>
<b>P53</b>			<0.001
Pattern NM	25 (42.4)	3 (5.5)	
Pattern BP	16 (27.1)	3 (5.5)	
Pattern HI	14 (23.7)	39 (70.9)	
Pattern NS	4 (6.8)	10 (18.2)	
<b>Ki-67</b>			<0.001
Pattern NM	8 (13.6)	2 (3.6)	
Pattern BP	30 (50.8)	10 (18.2)	
Pattern HI	21 (35.6)	43 (78.2)	
<b>Gender</b>			0.851
Male	48 (81.4)	43 (78.2)	
Female	11 (18.6)	12 (21.8)	
<b>Age (mean (SD))</b>	60.39 (10.50)	64.53 (12.29)	0.055
<b>Location</b>			0.560
Larynx	30 (50.8)	24 (43.6)	
Oral cavity	29 (49.2)	31 (56.4)	
<b>Tobacco use</b>			0.547
Non-smoker	18 (30.5)	22 (40.0)	
Former smoker	20 (33.9)	15 (27.3)	
Current smoker	21 (35.6)	18 (32.7)	
<b>Alcohol consumption</b>			0.245
No history	24 (40.7)	31 (56.4)	
≤ 3 drinks per day	15 (25.4)	10 (18.2)	
> 3 drinks per day	20 (33.9)	14 (25.5)	
<b>BMI</b>	24.22 (3.24)	23.54 (4.43)	0.349
<b>DM</b>			0.819
Yes	15 (25.4)	16 (29.1)	
No	44 (74.6)	39 (70.9)	

ND: non-dysplasia; LGD: low grade dysplasia; HGD: high grade dysplasia; SqCC: squamous cell carcinoma; SD: standard deviation.



**Table 3. Univariable and multivariable analysis of p53 and Ki-67 for predicting HGD and SqCC.**

	Univariable		Multivariable	
	OR (95% CI)	P value	OR (95% CI)	P value
<b>P53</b>				
Pattern BP	1.64 (0.28-9.58)	0.846	1.77 (0.27-11.60)	0.551
Pattern HI	18.00 (4.28-75.69)	< 0.001	8.68 (1.84-40.98)	0.006
Pattern LS	9.00 (1.55- 52.27)	0.014	7.66 (1.12-52.53)	0.038
<b>Ki-67</b>				
Pattern BP	2.00 (0.20-19.91)	0.554	2.70 (0.22-32.92)	0.437
Pattern HI	18.86 (2.15-165.28)	0.008	10.63 (1.00-112.41)	0.049

OR: odds ratio; CI: confidence interval; HGD: high grade dysplasia; SqCC: squamous cell carcinoma.

### **Development for scoring system based on logistic regression analysis**

Based on logistic regression analysis, a scoring system as a predictive model was developed using the p53 and Ki-67 expression patterns (Table 4). Fig 5 presents the relative importance of each variable in the logistic regression analysis. According to variable importance, the p53 expression pattern score was 0, 2, or 3 for pattern NM or BP, pattern LS, or pattern HI, respectively. The score of Ki-67 expression pattern was 0 or 1 for pattern NM or BP, and pattern HI, respectively.

The mean scores of two groups between ND & LGD and HGD & SqCC were  $1.17 \pm 0.241$  and  $3.23 \pm 0.206$ , respectively (Fig. 4). Between two groups, there was a statistically significant difference and clearly, the HGD & SqCC groups showed high scores ( $P < 0.001$ ).

On test data, comparisons of the classification efficiency of developed predictive models with various cut-off values were conducted (Table 5). When the cut-off value was set to two points, the accuracy, sensitivity, and specificity were 0.846,

0.706, and 1.000, respectively, which were the most efficient values ( $P < 0.001$ ). The AUC of cut-off 2 was the largest (0.853,  $P < 0.001$ ), which was consistent with previous analysis.

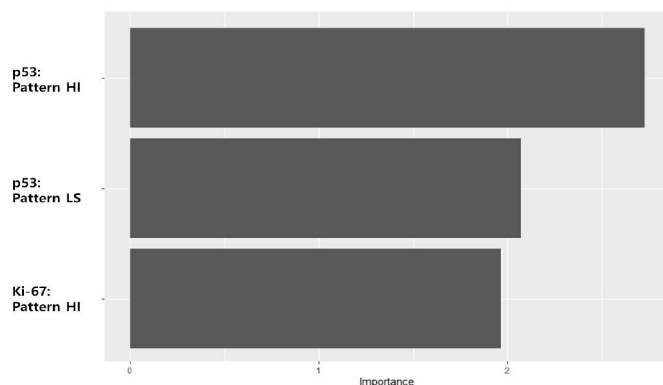


**Figure 5. Variable importance in logistic regression analysis.**

**Table 4. Parameters and scoring points of scoring system.**

	Points scored
<b>P53 expression pattern</b>	
Pattern NM	0
Pattern BP	0
Pattern HI	3
Pattern LS	2
<b>Ki-67 expression pattern</b>	
Pattern NM	0
Pattern BP	0
Pattern HI	1
<b>Total maximum score</b>	<b>4</b>

**Table 5. Comparisons of the classification efficiency of the two cut-off points**

Cut-off	Accuracy	95% CI	AUC	Sensitivity	Specificity	<i>P</i>
2	0.846	0.681-0.949	0.853	0.706	1.000	< 0.001
3	0.818	0.645-0.930	0.822	0.706	0.937	< 0.001

CI: confidence interval; AUC: The area under receiver operating characteristic curve.

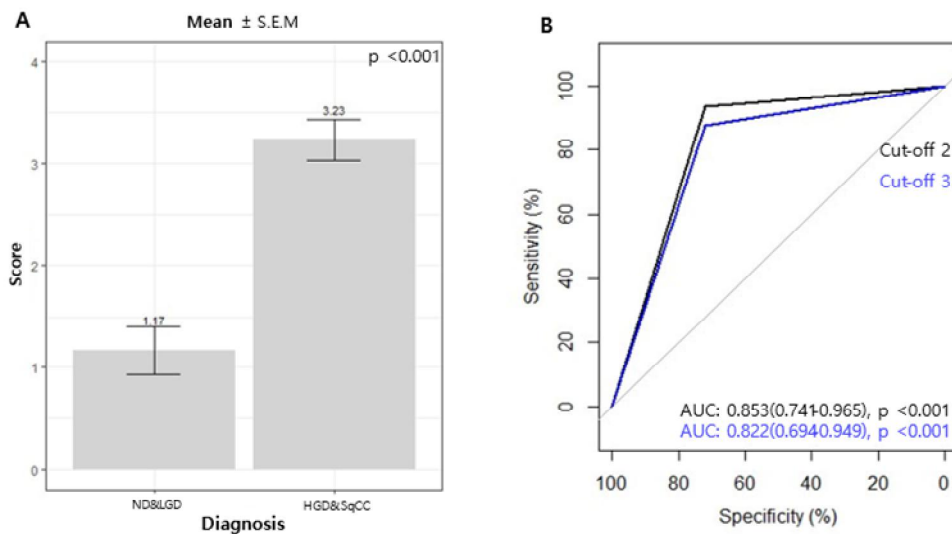


**Figure 6. The mean and AUC of two groups for a scoring system: ND or LGD, HGD or SqCC.** A. The mean scores of two groups are  $1.41 \pm 0.250$  and  $3.23 \pm 0.206$  (mean  $\pm$  S.E.M) respectively ( $P < 0.001$ ). B. The receiver operating characteristic (ROC) curves for two cut-off values were analyzed. ND: non-dysplasia; LGD: low grade dysplasia; HGD: high grade dysplasia; SqCC: squamous cell carcinoma; AUC, The area under ROC curve.

### Decision tree analysis

Constructed decision tree model using 81 cases of training set proposed p53 as the most important markers for differentiating group 1 and group 2 (Fig. 5A). When p53 expression is pattern NM or BP, the lesion was classified as ND or LGD

(29/35, 82.9%). The squamous epithelial lesion expressing pattern HI or LS for p53 was classified as HG or SqCC (33/46, 71.7%). The accuracy and AUC were 84.9% and 0.85, respectively.

The cohort was reclassified into three categories: non-dysplasia (ND), LGD, and the aforementioned group, group 2 with HGD or SqCC. For the aim of differentiating ND, LGD, group 2 including HGD or SqCC, decision tree model constructed using the training set suggested that p53 and Ki-67 were important markers (Fig. 5B). When differentiating epithelial lesions into three groups, the most critical marker was the p53 expression pattern, and lesions were classified first according to their p53 expression pattern. Among lesions expressing the pattern NM or BP for p53 (35 cases), 18 cases showed pattern NM or BP for Ki-67 and were classified as ND (18/25, 72%). The lesion showed pattern NM or BP for p53 and pattern HI for Ki-67 and were classified as LGD (6/10, 60%). The lesions expressing the pattern HI, or LS for p53 were classified as group 2 including HGD or SqCC (34/47, 72.3%). The accuracy and AUC were 75% ( $P = 0.004$ ) and 0.87, respectively, according to the internal validation.

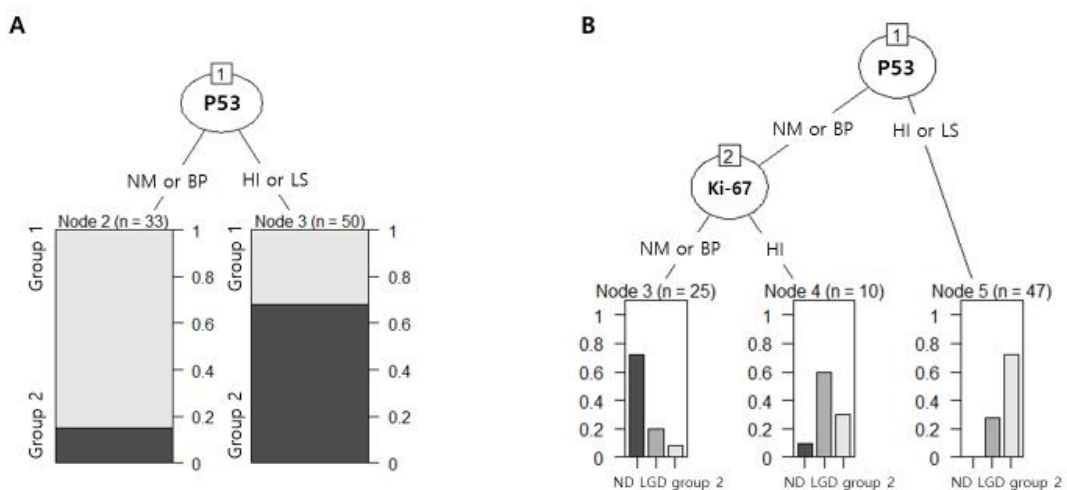


**Figure 7. Decision tree models to differentiate epithelial lesion.** A. A decision tree

model to differentiate two groups: group 1 (ND or LGD) and group 2 (HGD or SqCC). B. A decision tree model to differentiate ND, LGD, and group 2 (HGD or SqCC). ND, not-dysplasia; LGD, Low grade squamous dysplasia; HGD, High grade squamous dysplasia; SqCC, squamous cell carcinoma; D, squamous dysplasia; NM, pattern NM; BP, pattern BP; HI, pattern HI; LS, pattern LS.

### Interobserver variability in diagnosis

The interobserver variability for a pair of raters (J.S.S versus J.S.J) was conducted using the Cohen Kappa statistic. The results for interobserver variability with diagnosis based on H&E slide and the integrated diagnosis using H&E slide and IHC for p53 and Ki-67 are present in Table 6. The correlation was substantial for diagnosis based on H&E slides (weighted kappa 0.80, unweighted kappa 0.67). The integrated diagnosis had a better correlation with near perfect agreement (weighted kappa 0.92, unweighted kappa 0.88). Five cases initially diagnosed as LGD on the H&E slide were changed to HGD on the integrated diagnosis using IHC for p53 and Ki-67 (Fig. 6). The IHC for p53 and Ki-67 assisted the binary grading of epithelial lesions with intermediate atypia.

**Table 6. Kappa scores for diagnosis based on H&E slide and the integrated diagnosis (95% confidence interval)**

	<i>kappa</i>	
	Diagnosis based on H&E slide	The integrated diagnosis
Unweighted	0.67 (0.57-0.77)	0.88 (0.81-0.95)
Weighted	0.80 (0.74-0.86)	0.92 (0.87-0.96)

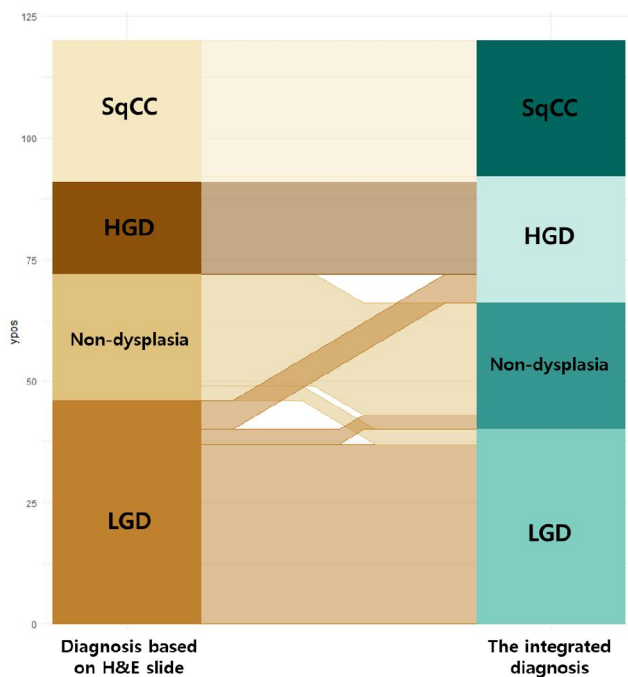


**Figure 8. Changes between diagnosis based on H&E slide and the integrated diagnosis.** LGD, Low grade squamous dysplasia; HGD, High grade dysplasia; SqCC, squamous cell carcinoma.

### ***TP53* mutational analysis and correlation with p53 expression**

*TP53* mutations were detected using NGS in 16 cases of SqCC (Table 6). Three cases harbored two mutations, for a total of 19 mutations. The most frequent mutation was missense mutation (11/19, 57.9%), followed by frameshift mutation (4/19, 21.1%), nonsense mutation (3/19, 15.8%), and splicing site mutation (1/19, 5.3%). Most of these mutations were located in DNA-binding domain (17/19, 89.5%), but one mutation was in N-terminal domain (1/19, 5.3%) and another mutation was in C-terminal domain (1/19, 5.3%).

*TP53* mutation analysis was integrated with p53 and Ki-67 expression analysis to develop a comprehensive genomic profile (Fig. 6). In total, 16 cases showed

patterns BP, HI, and LS, but not NM. Fifteen of 16 cases (93.8%) exhibited pattern HI or LS. Five of five cases (100%) expressing pattern LS for p53 had nonsense or frameshift mutation. Nine of ten cases (90%) exhibiting pattern HI for p53 had missense mutation.

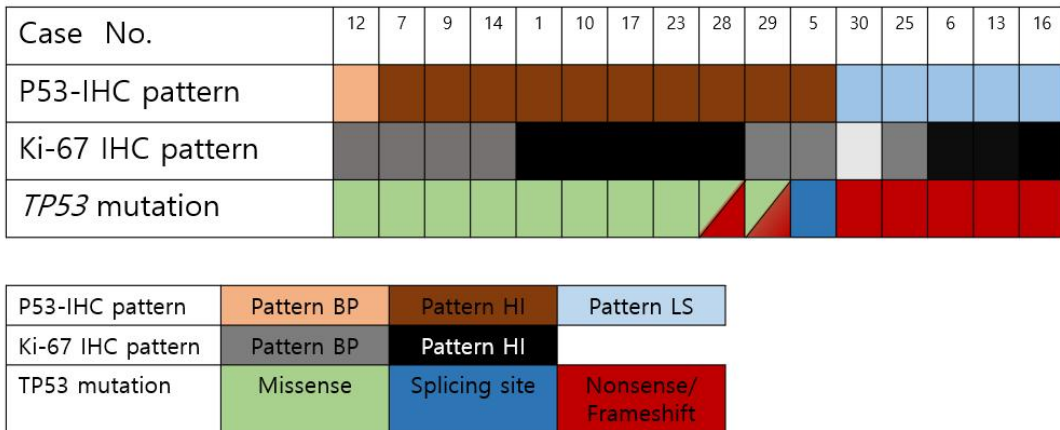


**Figure 9. comprehensive TP53 genomic profile of SqCC.** The expression patterns of p53 and KI-67 and mutation types of TP53 are colored by the column indicated in the left lower side.

**Table 7. TP53 mutation in SqCC.**

Case No.	Amino acid Alteration	Type	Allele frequency	P53 expression pattern	Ki-67 expression pattern
1	C176F	SNV	0.81	HI	HI
5	X307_splice alteration	DEL	0.23	HI	BP
6	K139Afs*4	DEL	0.59	LS	HI
7	Y205C	SNV	0.86	HI	BP
10	D259N	SNV	0.35	HI	HI

	MA160IS	DNP	0.66		
12	R158H	SNV	0.74	BP	BP
13	P190Lfs*57	DEL	0.62	LS	HI
14	R273H	SNV	0.56	HI	BP
16	D48Gfs*4	INS	0.57	LS	HI
17	R175H	SNV	0.11	HI	HI
23	R273H	SNV	0.33	HI	HI
25	C229*	INS	0.05	LS	BP
28	R248Q	SNV	0.21	HI	HI
	R196*	SNV	0.29		
29	P278L	SNV	0.32	HI	BP
	R267Efs*4	DEL	0.16		
30	R280*	SNV	0.50	LS	NM

NM: pattern NM; BP: pattern BP; HI: pattern HI; LS: pattern LS.

### Prognosis of HGD and SqCC according to p53 expression patterns

Disease free survival (DFS) according to the expression patterns of p53 was evaluated in patients first diagnosed with HGD or SqCC (Fig. 7). In SqCC, the average follow-up period was 16.7 months (range: 2-34 months). Twelve of 19 cases (63.2%) recurred following treatments. Although there was also no statistically significant difference in DFS according to p53 expression patterns, there was a tendency for recurrence when the lesion showed the pattern LS or HI for p53 ( $P = 0.14$ ). In HGD, the average follow-up period was 16.3 months



(range: 0-29 months). Two of 18 cases (11.1%) recurred HGD and one case (5.6%) progressed to SqCC following treatments. As with SqCC, there was no statistical difference, but there was a tendency for recurrence when the lesion showed the pattern LS or HI for p53 ( $P = 0.24$ ).

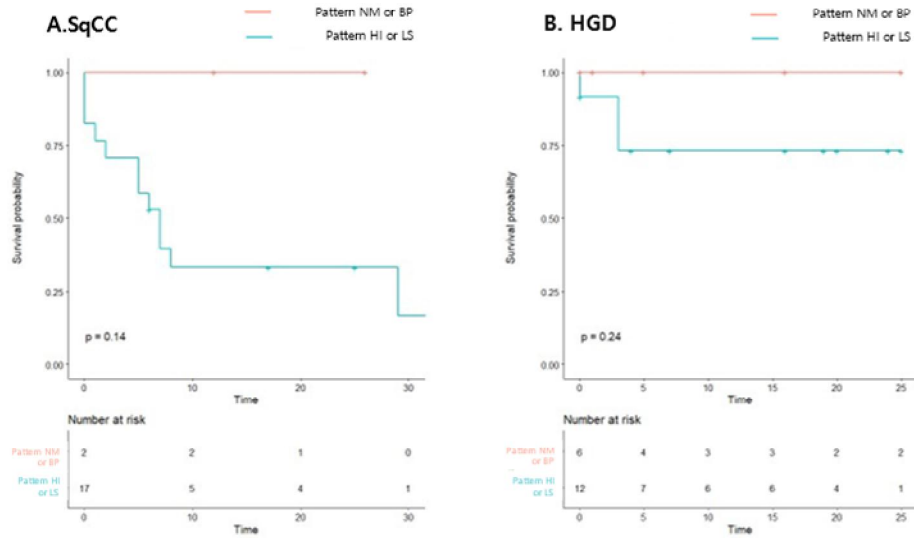


**Figure 10. Disease free survival of SqCC and HGD according to p53 expression patterns.** A. DFS of SqCC ( $P = 0.14$ ). B. DFS of HGD ( $P = 0.24$ ). DFS: disease free survival; SqCC: squamous cell carcinoma; HGD: high grade dysplasia.

## Discussion

The scoring system and decision tree models were developed to differentiate oral and laryngeal epithelial lesions using IHC for p53 and Ki-67. In logistic regression analysis and decision tree models constructed to differentiate two groups of epithelial lesions (ND or LGD versus HGD or SqCC), p53 is a critical marker. The epithelial lesions with pattern HI or LS for p53 can be classified as HGD or SqCC. If the epithelial lesions with ambiguous cytological and architectural atypia to diagnose with HGD or SqCC express the pattern HI or LS for p53, it is recommended to diagnose HGD or SqCC.

Evaluation of p53 expression pattern is one of the most frequently suggested method to overcome the limitations inherent in diagnosing dysplasia solely based on morphologic findings. In recent large studies, *TP53* mutations are most frequently detected in HNSCC, including the oral cavity and larynx. As a founder event, the *TP53* mutation is regarded as an early step in carcinogenesis (1, 2). Sawada *et al.* confirmed pattern HI and LS were significantly associated with *TP53* mutations, especially missense and nonsense mutations, respectively, which was consistent with this study (Fig. 6). Six of 14 oral squamous cell dysplasia cases with pattern HI or LS had *TP53* mutation and progressed to SqCC without further treatment (9).

Since the methods for analyzing p53 IHC varied between studies, it was difficult to compare the results of this study to those of the previous studies. In previous research analyzing p53 expression patterns in oral epithelial dysplasia, there were three p53 expression patterns: basal pattern, limited p53-positive cells in the basal layer which similar to patterns NM and BP; negative pattern, loss of expression for p53 which similar to pattern LS; and suprabasal, similar to pattern HI. Oral epithelial dysplasia expressing negative or suprabasal patterns for p53

were associated with progression to SqCC as compared to basal pattern for p53 (38). SqCC immunopositive for p53 was significantly associated with recurrence in other study that analyzed p53 expression using a cutoff value of 10% (39). In this study, there was a tendency for recurrence when the lesion showed the pattern LS or HI for p53.

Whereas Sawada *et al.* used antibody against p53, PAb 1801, the data obtained from this study using DO-7 are comparable with theirs. Because both antibodies recognize the N-terminal region of p53 and mutations in this region are rare, both antibodies react with p53 protein regardless of mutations. Furthermore, several studies have demonstrated that there is no significant difference in the sensitivity and specificity of the two antibodies (40, 41), as well as no difference in the presence or absence of staining regardless of the *TP53* mutation (40).

Proliferating cells immunoreactive for Ki-67 as a proliferating marker are restricted to the basal and parabasal layer and mainly the parabasal layer in normal oral and laryngeal epithelium due to the asymmetric cell division of the epithelial stem cell located in the basal layer. Because of the loss of asymmetric cell division, the functions of stem cells are altered, and stem cells are replaced by proliferating cells, which increase in number not only in the parabasal layer, but also in the basal and suprabasal layers in epithelial dysplasia (21). Ki-67 labeling index was proposed as a diagnostic marker due to its ability to detect structural alteration in the distribution of proliferating cells and stem cells in epithelial dysplasia (19, 21, 42).

Previous studies have revealed different results regarding the relationship between the Ki-67 labeling index (LI) and epithelial dysplasia and SqCC. In some studies, the Ki-67 LI increases according to the degree of epithelial dysplasia and SqCC (19, 21). Birajdar *et al.*, on the other hand, compared the average of oral

epithelial lesions by Ki-67 LI and observed that the average of HGD was significantly greater than that of SqCC. In well-differentiated SqCC, mitosis was frequently observed in peripheral lesions that were less differentiated, and there were more proliferating cells immunoreactive for Ki-67 in the peripheral lesions than in the center, which was highly differentiated and capable of keratinization. The more advanced degree of dysplasia, more cells immunopositive for Ki-67 were observed in the central portion of lesion (42). Although the mean of Ki-67 LI was not analyzed, the frequency of pattern HI was greater in HGD than in SqCC.

Because the increased number of Ki-67 positive cells in suprabasal layer according to the degree of the epithelial dysplasia, the expression pattern of Ki-67 rather than the Ki-67 LI was used to intuitively evaluate the altered architecture of proliferating cells and stem cells. Ki-67 was not a significant marker to differentiate two groups: non-dysplasia or LGD, HGD or SqCC. However, in another decision tree model to differentiate three groups of epithelial lesions (ND, LGD, and group 2 including HGD or SqCC), Ki-67 is an important diagnostic marker.

The cases which had pattern HI for Ki-67 and pattern NM or BP for p53 included one case of ND, ten cases of LGD, and three cases of HGD. The frequency of pattern HI for Ki-67 increased with HGD and SqCC, and the relationship between p53 and Ki-67 was very weakly linear. When epithelial lesions have pattern HI for Ki-67 and pattern NM or BP for p53, totaling 1 point, and equivocal morphological atypia, it is recommended to diagnose as "epithelial lesion of unknown significance" rather than "reactive lesion" for conducting re-biopsy or longer follow-up.

There were seven cases of LGD, one case of HGD, and two cases of SqCC which

had pattern NM or BP for p53 and Ki-67. In one of the discrepancy cases, the presence of architectural atypia, including an abnormally located keratin pearl, and mild cytologic atypia supported the diagnosis of LGD, despite the decision tree model classifying the LGD case as ND (Fig. 8). The assessment was restricted due to the fragmented and small biopsy specimen. Following excisional biopsy, SqCC was identified, suggesting that the discrepancy between the first and second biopsies was likely due to the fragmented and small specimen and sampling error.

There were one case of ND and three cases of HGD with pattern NM or BP for p53 and pattern HI for Ki-67. In ND case, the lesion showed the cytologic and architectural changes including minimally increased nuclei and basal hyperplasia (Fig. 9). However, the presence of a prominent nucleoli with smooth nuclear membrane and intraepithelial inflammation suggested that the inflammation resulted in these changes. In the HGD case, despite the discrepancy with the decision tree model, cytologic and architectural atypia were evident, supporting the diagnosis (image not shown).

Eighteen cases of LGD and two cases of ND had pattern HI or LS for p53 and were classified as HGD or SqCC by the scoring system and decision tree models. In one of LGD cases, atypical cells with mild pleomorphism occupied in lower half of the epithelium, insufficient to diagnose HGD (Fig. 10). In one of ND cases, there was no cytologic and architectural atypia, despite the results of p53 IHC (Fig. 11). All ND cases with discrepancies showed pattern HI, while pattern LS was absent.

Despite the discrepancy between the diagnosis based on histologic criteria and classification by the scoring system and decision tree models, the integrated diagnosis using morphologic features and IHC for p53 and Ki-67 improved

correlation and agreement. In the past decades, many histologic-based grading systems for squamous intraepithelial lesions have been proposed to improve diagnostic reproducibility and accuracy. However, the WHO 2017 diagnostic criteria for laryngeal epithelial dysplasia cannot clearly distinguish LGD from basal hyperplasia (43). Oral epithelial lesion interpretation remained difficult and interobserver variability persisted, due to the complexity of the WHO 2017 classification's grading system for oral epithelial dysplasia (14, 16, 17, 43). The integrated diagnostic system combining histologic features and IHC for p53 and Ki-67 aid more accurate diagnosis and improve reproducibility.

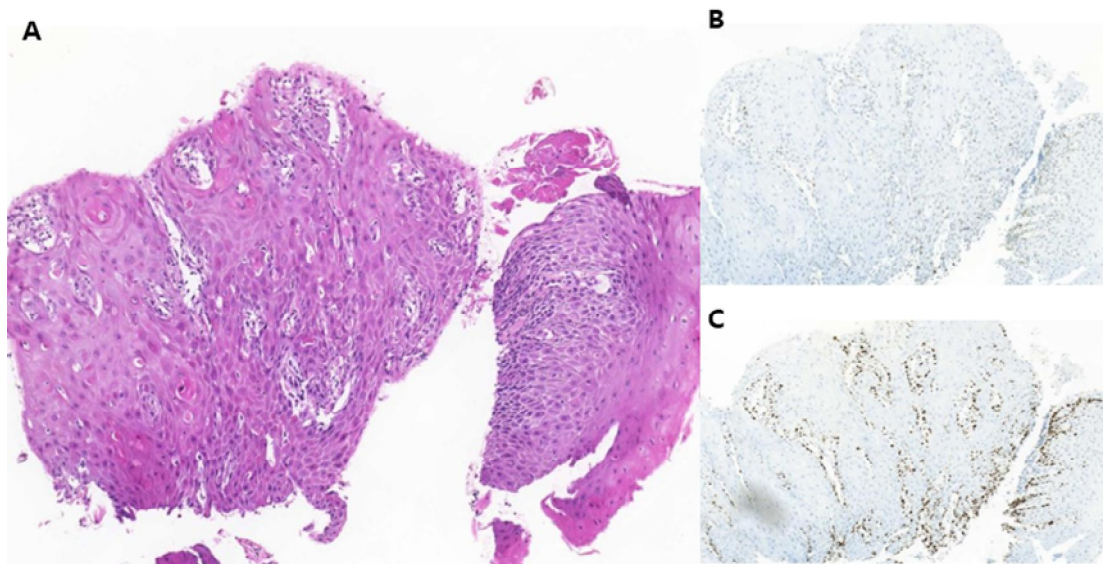


**Figure 11. The first case of discrepancy between diagnosis based on H&E slide and classification by decision tree model. A. morphologic features of oral epithelial lesion (H&E slide, 10X), B. Pattern NM for p53 (10X). C. Pattern Base for Ki-67 (10X).**

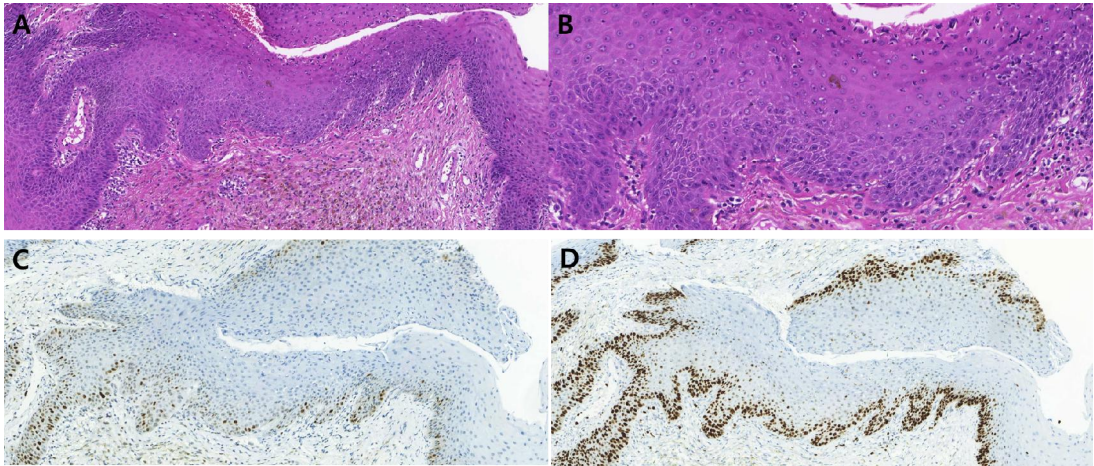


**Figure 12. The second case of discrepancy between diagnosis based on H&E slide and classification by decision tree model. A & B. morphologic features of laryngeal epithelial lesion (H&E slide, A. 10X; B. 20X), B. Pattern NM for p53 (10X). C. pattern HI for Ki-67 (10X).**

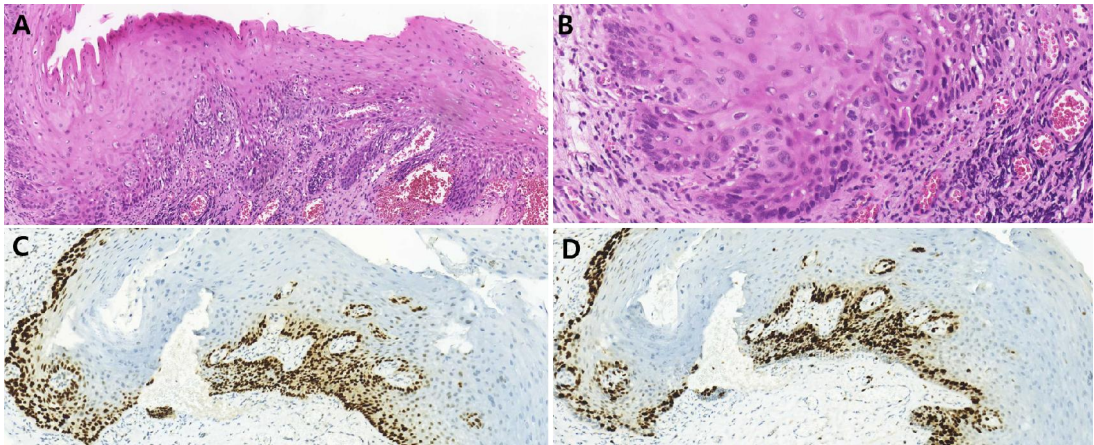


**Figure 13. The third case of discrepancy between diagnosis based on H&E slide and classification by decision tree model. A & B. morphologic features of oral epithelial lesion (H&E slide, A. 10X B. 20X), B. Pattern HI for p53 (10X). C. pattern HI for Ki-67 (10X).**

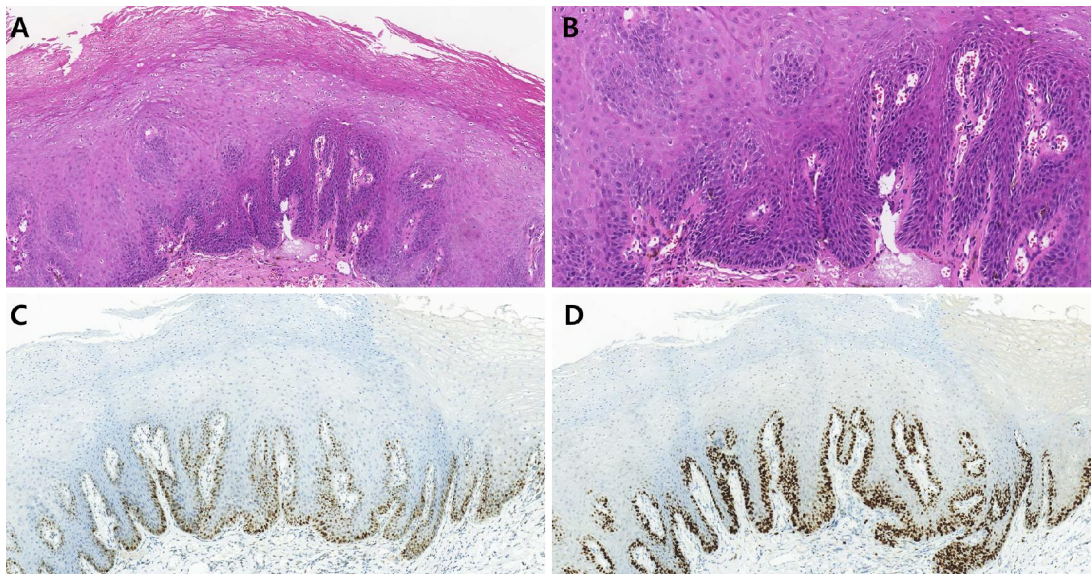


**Figure 14. The fourth case of discrepancy between diagnosis based on H&E slide and classification by decision tree model.** A & B. morphologic features of oral epithelial lesion (H&E slide, A. 10X; B. 20X), B. Pattern HI for p53 (10X). C. pattern HI for Ki-67 (10X).

In a few cases, morphological findings alone are insufficient to explain the biological behavior of the lesion. There have been reports that lesions of benign hyperkeratosis progressed to invasive SqCC in 1% to 30% of cases (44-47). Proliferative verrucous leukoplakia, which has a 70% probability of progressing malignancy, may show hyperkeratosis with minimal to no atypia (48, 49). It was proposed to diagnose lesion that is not reactive but does not have cytological atypia as "keratosis of unknown significance (KUS)" rather than reactive epithelial change (50). Genetic alteration in *KMT2C* (75%) and *TP53* (35%) were detected in oral epithelial dysplasia and KUS, supporting the hypothesis that KUS is initial event of development of SqCC (51).

However, interobserver variability is to be expected, because KUS is diagnosed by morphological criteria. Objective information provided by IHC markers such as p53 and Ki-67 may be required. It is suggested that analyzing the p53 and Ki-67



expression patterns in KUS will improve diagnostic accuracy and the predictive model for differentiating ND, D, and SqCC.

There are several limitations of this study. First, the study cohort was small and constituted of only one institution. Although the performance of predictor models developed by decision tree algorithm was good, it could be due to its small size. Additionally, the predictor model may be overfitted in this study cohort. Further research in a larger study may be necessary for optimizing and external validation of the decision tree model. Second, because most patients diagnosed ND or LGD were not followed up, the prognosis of ND or LGD could not be assessed according to the expression patterns of p53 or Ki-67. Third, the NGS was performed on some SqCC cases, not on the entire cohort that developed the scoring system and decision tree models.

### **Conclusion**

The correlation between the *TP53* mutation and the expression patterns of p53 was confirmed and the predictive models of diagnosis was developed. Therefore, the scoring system based on p53 and Ki-67 expression patterns aids the differentiation of epithelial lesions, especially when the morphologic features are ambiguous.

## References

1. Zhou G, Liu Z, Myers JN. TP53 Mutations in Head and Neck Squamous Cell Carcinoma and Their Impact on Disease Progression and Treatment Response. *J Cell Biochem.* 2016;117(12):2682-92.
2. Network TCGA. Comprehensive genomic characterization of head and neck squamous cell carcinomas. *Nature.* 2015;517(7536):576-82.
3. Blons H, Laurent-Puig P. TP53 and head and neck neoplasms. *Hum Mutat.* 2003;21(3):252-7.
4. Shi Q, Xiao K, Wei W, Zhang B-Y, Chen C, Xu Y, et al. Associations of TP53 mutations, codon 72 polymorphism and human papillomavirus in head and neck squamous cell carcinoma patients. *Oncology reports.* 2013;30(6):2811-9.
5. Shahnava SA, Regezi JA, Bradley G, Dubé ID, Jordan RC. p53 gene mutations in sequential oral epithelial dysplasias and squamous cell carcinomas. *J Pathol.* 2000;190(4):417-22.
6. Ogmundsdóttir HM, Björnsson J, Holbrook WP. Role of TP53 in the progression of pre-malignant and malignant oral mucosal lesions. A follow-up study of 144 patients. *J Oral Pathol Med.* 2009;38(7):565-71.
7. Kusama K, Okutsu S, Takeda A, Himiya T, Kojima A, Kidokoro Y, et al. p53 gene alterations and p53 protein in oral epithelial dysplasia and squamous cell carcinoma. *J Pathol.* 1996;178(4):415-21.
8. Graveland AP, Bremmer JF, de Maaker M, Brink A, Cobussen P, Zwart M, et al. Molecular screening of oral precancer. *Oral Oncol.* 2013;49(12):1129-35.
9. Sawada K, Momose S, Kawano R, Kohda M, Irié T, Mishima K, et al. Immunohistochemical staining patterns of p53 predict the mutational status of TP53 in oral epithelial dysplasia. *Modern Pathology.* 2022;35(2):177-85.
10. Johnson DE, Burtneess B, Leemans CR, Lui VWY, Bauman JE, Grandis JR. Head and neck squamous cell carcinoma. *Nat Rev Dis Primers.* 2020;6(1):92.
11. El-Naggar AK, Chan JK, Grandis JR. WHO classification of head and neck tumours 2017.

12. Fischer DJ, Epstein JB, Morton TH, Schwartz SM. Interobserver reliability in the histopathologic diagnosis of oral pre-malignant and malignant lesions. *J Oral Pathol Med.* 2004;33(2):65-70.
13. Fleskens SA, Bergshoeff VE, Voogd AC, van Velthuysen ML, Bot FJ, Speel EJ, et al. Interobserver variability of laryngeal mucosal premalignant lesions: a histopathological evaluation. *Mod Pathol.* 2011;24(7):892-8.
14. Mehlum CS, Larsen SR, Kiss K, Groentved AM, Kjaergaard T, Möller S, et al. Laryngeal precursor lesions: Interrater and intrarater reliability of histopathological assessment. *Laryngoscope.* 2018;128(10):2375-9.
15. Karabulut A, Reibel J, Therkildsen MH, Praetorius F, Nielsen HW, Dabelsteen E. Observer variability in the histologic assessment of oral premalignant lesions. *J Oral Pathol Med.* 1995;24(5):198-200.
16. Tilakaratne WM, Jayasooriya PR, Jayasuriya NS, De Silva RK. Oral epithelial dysplasia: Causes, quantification, prognosis, and management challenges. *Periodontol 2000.* 2019;80(1):126-47.
17. Mahmood H, Bradburn M, Rajpoot N, Islam NM, Kujan O, Khurram SA. Prediction of malignant transformation and recurrence of oral epithelial dysplasia using architectural and cytological feature specific prognostic models. *Modern Pathology.* 2022.
18. Chen S, Forman M, Sadow PM, August M. The Diagnostic Accuracy of Incisional Biopsy in the Oral Cavity. *Journal of Oral and Maxillofacial Surgery.* 2016;74(5):959-64.
19. Mondal D, Saha K, Datta C, Chatterjee U, Sengupta A. Ki67, p27 and p53 Expression in Squamous Epithelial Lesions of Larynx. *Indian J Otolaryngol Head Neck Surg.* 2013;65(2):126-33.
20. Dragomir LP, Simionescu C, Mărgăritescu C, Stepan A, Dragomir IM, Popescu MR. P53, p16 and Ki67 immunoexpression in oral squamous carcinomas. *Rom J Morphol Embryol.* 2012;53(1):89-93.
21. Takeda T, Sugihara K, Hirayama Y, Hirano M, Tanuma JI, Semba I. Immunohistological evaluation of Ki-67, p63, CK19 and p53 expression in oral

- epithelial dysplasias. *J Oral Pathol Med.* 2006;35(6):369-75.
22. Kujan O, Oliver RJ, Khattab A, Roberts SA, Thakker N, Sloan P. Evaluation of a new binary system of grading oral epithelial dysplasia for prediction of malignant transformation. *Oral Oncol.* 2006;42(10):987-93.
23. Wagle N, Berger MF, Davis MJ, Blumenstiel B, Defelice M, Pochanard P, et al. High-throughput detection of actionable genomic alterations in clinical tumor samples by targeted, massively parallel sequencing. *Cancer Discov.* 2012;2(1):82-93.
24. Kim JH, Yoon S, Lee DH, Jang SJ, Chun SM, Kim SW. Real-world utility of next-generation sequencing for targeted gene analysis and its application to treatment in lung adenocarcinoma. *Cancer Med.* 2021;10(10):3197-204.
25. Jeong J-S, Cho K-J, Kim D, Lee YS, Song JS. Genomic alteration in rare subtype of sarcomatoid salivary duct carcinoma. *Pathology - Research and Practice.* 2021;228:153678.
26. Li H, Durbin R. Fast and accurate short read alignment with Burrows–Wheeler transform. *Bioinformatics.* 2009;25(14):1754-60.
27. McKenna A, Hanna M, Banks E, Sivachenko A, Cibulskis K, Kernytzky A, et al. The Genome Analysis Toolkit: a MapReduce framework for analyzing next-generation DNA sequencing data. *Genome Res.* 2010;20(9):1297-303.
28. Cibulskis K, Lawrence MS, Carter SL, Sivachenko A, Jaffe D, Sougnez C, et al. Sensitive detection of somatic point mutations in impure and heterogeneous cancer samples. *Nature Biotechnology.* 2013;31(3):213-9.
29. Sherry ST, Ward MH, Kholodov M, Baker J, Phan L, Smigielski EM, et al. dbSNP: the NCBI database of genetic variation. *Nucleic Acids Research.* 2001;29(1):308-11.
30. McLaren W, Pritchard B, Rios D, Chen Y, Flicek P, Cunningham F. Deriving the consequences of genomic variants with the Ensembl API and SNP Effect Predictor. *Bioinformatics.* 2010;26(16):2069-70.
31. Gehring JS, Fischer B, Lawrence M, Huber W. SomaticSignatures: inferring mutational signatures from single-nucleotide variants. *Bioinformatics.*

2015;31(22):3673-5.

32. Lawrence MS, Stojanov P, Polak P, Kryukov GV, Cibulskis K, Sivachenko A, et al. Mutational heterogeneity in cancer and the search for new cancer-associated genes. *Nature*. 2013;499(7457):214-8.

33. Cerami E, Gao J, Dogrusoz U, Gross BE, Sumer SO, Aksoy BA, et al. The cBio Cancer Genomics Portal: An Open Platform for Exploring Multidimensional Cancer Genomics Data. *Cancer Discovery*. 2012;2(5):401-4.

34. Talevich E, Shain AH, Botton T, Bastian BC. CNVkit: Genome-Wide Copy Number Detection and Visualization from Targeted DNA Sequencing. *PLOS Computational Biology*. 2016;12(4):e1004873.

35. Kuhn M. Building Predictive Models in R Using the caret Package. *Journal of Statistical Software*. 2008;28(5):1 - 26.

36. Gale N, Blagus R, El-Mofty SK, Helliwell T, Prasad ML, Sandison A, et al. Evaluation of a new grading system for laryngeal squamous intraepithelial lesions--a proposed unified classification. *Histopathology*. 2014;65(4):456-64.

37. Chaturvedi AK, Udaltsova N, Engels EA, Katznel JA, Yanik EL, Katki HA, et al. Oral Leukoplakia and Risk of Progression to Oral Cancer: A Population-Based Cohort Study. *J Natl Cancer Inst*. 2020;112(10):1047-54.

38. Cruz IB, Snijders PJ, Meijer CJ, Braakhuis BJ, Snow GB, Walboomers JM, et al. p53 expression above the basal cell layer in oral mucosa is an early event of malignant transformation and has predictive value for developing oral squamous cell carcinoma. *J Pathol*. 1998;184(4):360-8.

39. Shin DM, Lee JS, Lippman SM, Lee JJ, Tu ZN, Choi G, et al. p53 Expression: Predicting Recurrence and Second Primary Tumors in Head and Neck Squamous Cell Carcinoma. *JNCI: Journal of the National Cancer Institute*. 1996;88(8):519-29.

40. Lavieille JP, Righini C, Reyt E, Brambilla C, Riva C. Implications of p53 alterations and anti-p53 antibody response in head and neck squamous cell carcinomas. *Oral Oncol*. 1998;34(2):84-92.

41. Horne GM, Anderson JJ, Tiniakos DG, McIntosh GG, Thomas MD, Angus B,

et al. p53 protein as a prognostic indicator in breast carcinoma: a comparison of four antibodies for immunohistochemistry. *Br J Cancer*. 1996;73(1):29-35.

42. Birajdar SS, Radhika M, Paremala K, Sudhakara M, Soumya M, Gadivan M. Expression of Ki-67 in normal oral epithelium, leukoplakic oral epithelium and oral squamous cell carcinoma. *J Oral Maxillofac Pathol*. 2014;18(2):169-76.

43. Cho K-J, Song JS. Recent Changes of Classification for Squamous Intraepithelial Lesions of the Head and Neck. *Archives of Pathology & Laboratory Medicine*. 2018;142(7):829-32.

44. Hsue SS, Wang WC, Chen CH, Lin CC, Chen YK, Lin LM. Malignant transformation in 1458 patients with potentially malignant oral mucosal disorders: a follow-up study based in a Taiwanese hospital. *J Oral Pathol Med*. 2007;36(1):25-9.

45. Cowan CG, Gregg TA, Napier SS, McKenna SM, Kee F. Potentially malignant oral lesions in northern Ireland: a 20-year population-based perspective of malignant transformation. *Oral Dis*. 2001;7(1):18-24.

46. Holmstrup P, Thorn JJ, Rindum J, Pindborg JJ. Malignant development of lichen planus-affected oral mucosa. *J Oral Pathol*. 1988;17(5):219-25.

47. Brouns E, Baart J, Karagozoglu K, Aartman I, Bloemena E, van der Waal I. Malignant transformation of oral leukoplakia in a well-defined cohort of 144 patients. *Oral Dis*. 2014;20(3):e19-24.

48. Bagan J, Scully C, Jimenez Y, Martorell M. Proliferative verrucous leukoplakia: a concise update. *Oral Dis*. 2010;16(4):328-32.

49. Cabay RJ, Morton TH, Jr., Epstein JB. Proliferative verrucous leukoplakia and its progression to oral carcinoma: a review of the literature. *J Oral Pathol Med*. 2007;36(5):255-61.

50. Woo SB, Grammer RL, Lerman MA. Keratosis of unknown significance and leukoplakia: a preliminary study. *Oral Surg Oral Med Oral Pathol Oral Radiol*. 2014;118(6):713-24.

51. Villa A, Hanna GJ, Kacew A, Frustino J, Hammerman PS, Woo SB. Oral keratosis of unknown significance shares genomic overlap with oral dysplasia.

Oral Dis. 2019;25(7):1707-14.

## 국문요약

### 연구배경 및 목적

구강 및 후두 상피 병변은 WHO의 조직학적 진단 기준에 따라 진단하는데 이는 진단의 병리의사 간 변동성을 유발할 수 있다. 상피 병변의 조직학적 소견이 모호한 경우 진단에 도움이 될 수 있는 면역조직화학검사를 기반한 통합 진단 접근법이 필요하다.

### 연구재료와 연구방법

서울아산병원에서 2018-2021년 사이에 수술적 치료 또는 조직 검사를 받은 104명의 환자의 구강과 후두 조직 114례를 대상으로 하였다. p53과 Ki-67을 이용한 면역조직화학검사를 시행하였다. 로지스틱 회귀 분석과 결정 나무 알고리즘을 사용하여 상피 병변을 진단하기 위한 점수 체계와 예측 모형을 개발하였다. 관찰자 간 변동성을 평가하기 위해서 코헨 카파 상관계수 분석을 시행하였다. 차세대 염기 서열분석과 면역조직화학검사를 통해 TP53 돌연변이와 p53의 발현 유형 간의 관련성을 분석하였다.

### 연구결과

p53에 대한 두 가지 발현 유형인 확산 발현 유형 (pattern HI)과 발현이 소실된 유형 (pattern LS), Ki-67에 대한 pattern HI는 고등급 이형성증 (HGD) 또는 편평세포암 (SqCC)과 통계적으로 유의하게 연관되었다. 상피 병변을 비이형성 (ND) 또는 저등급 이형성증 (LGD), HGD 또는 SqCC의 두 집단으로 분류한 후 p53과 Ki-67의 면역조직화학검사 결과에 기반한 점수 체계로 상피 병변을 분류하였을 때 정확도와 the area under a receiver operating characteristic curve (AUC)이 각각 84.6%와 0.85이었다. p53과 Ki-67의 발현 유형을 이용한 의사 결정 나무 모형은



상피 병변을 ND, LGD, SqCC 또는 HGD 를 포함한 집단으로 분류하였고, 정확도와 AUC 가 75%와 0.87 이었다. 두 병리의사간 진단 일치율을 비교하였을 때, 조직학적 소견과 면역조직화학검사 결과를 이용한 통합 진단에서 거의 완벽한 일치를 보였다 (가중 카파 계수 0.92, 비가중 카파 계수 0.88). p53 에 대한 pattern HI 와 LS 는 각각 missense mutation 과 nonsense/frameshift mutation 과 상관관계가 있었다.

## 결론

*TP53* 돌연변이와 p53 의 발현 유형 사이의 상관관계를 확인하고 진단의 예측 모형을 개발하였다. 따라서 구강과 후두의 상피 병변의 조직학적 소견이 모호한 경우, p53 과 Ki-67 발현 유형에 기반한 점수 체계는 상피 병변의 진단하는 시 도움을 줄 수 있다.